Oh

Pauline

A thesis presented for the degree of
Bachelor of Science (Honours) (Physics)

School of Physics
Department of Science
The University of Sydney
Australia
February 23, 2026

Supervisor: Prof. Jane Professor

Co-Supervisor: Dr. Jack Supervisor

Co-Supervisor: Mr. June Supervisor

Tous les fichiers svg :

Dedication

For those who hate looking at a template with 500 lines of code and an extra 300 lines commented out.

Declaration

Acknowledgements

Contents

List of Figures

List of Tables

Chapter 1

Introduction

1.1 Fermi gas preparation (+ Bose gas ?)

1.1.1 TC

Comment on increasing power in TC (thésard marc chesnais)

1.1.2 Zeeman cooling

1.1.3 Blue MOT

1.1.3.1 The physics

1.1.3.2 How to optimize the superposition with the repumper

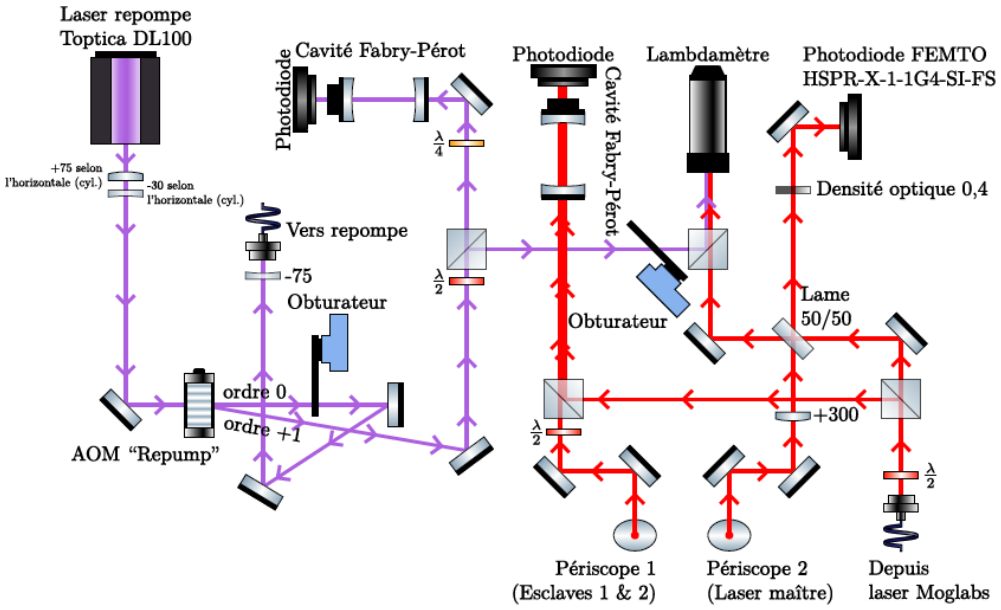

Figure 1.1: Caption

1.1.3.3 Comment on the hyperfine states (+boson 88)

1.1.3.4 Optical setup (blue + repump)

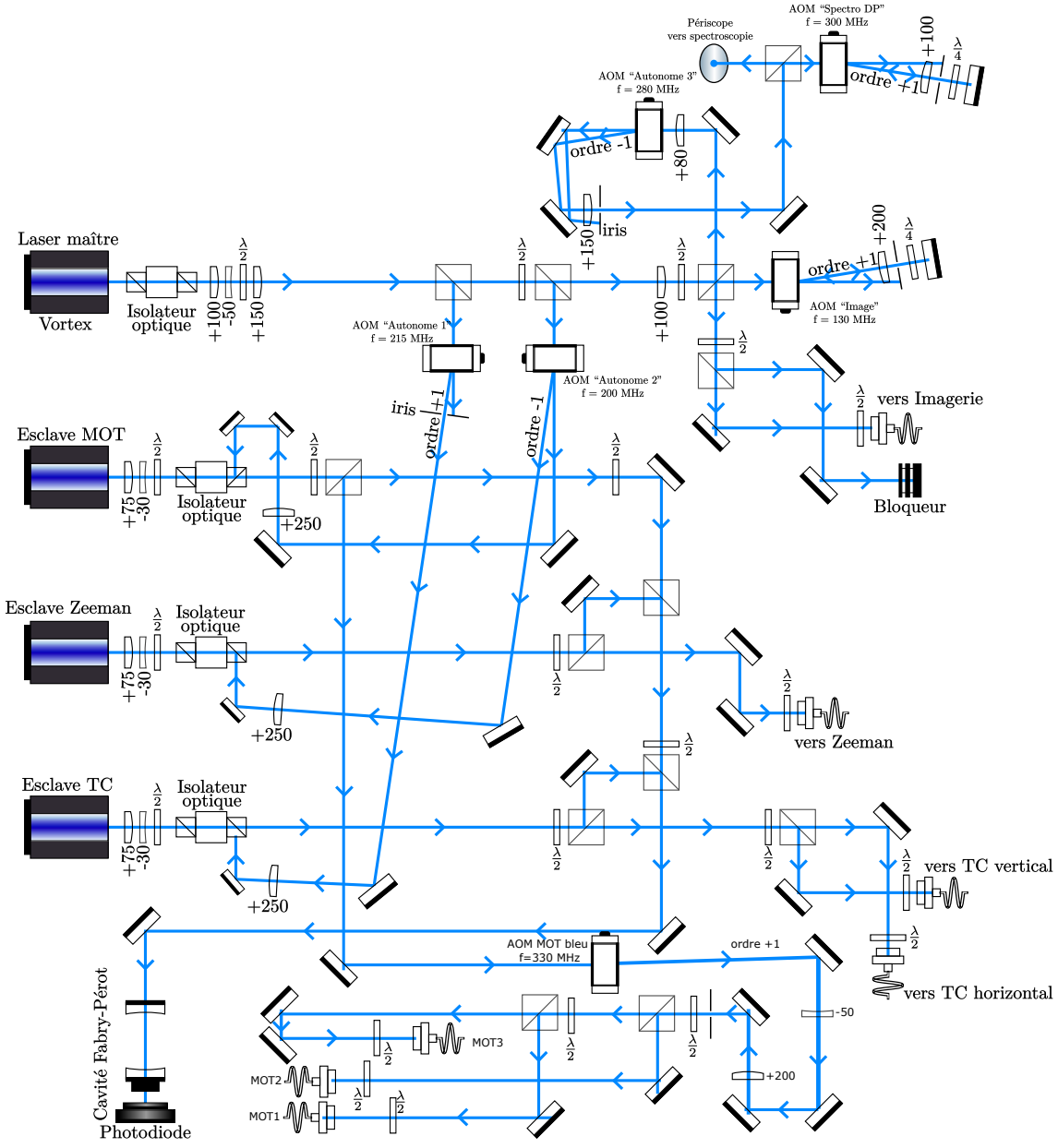

Figure 1.2: Caption

1.1.4 Repumper

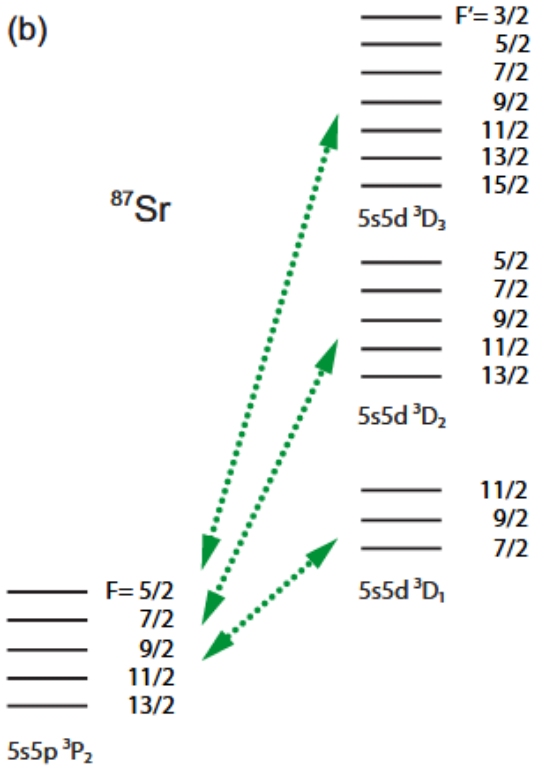

Figure 1.3: Caption

1.1.5 BB MOT

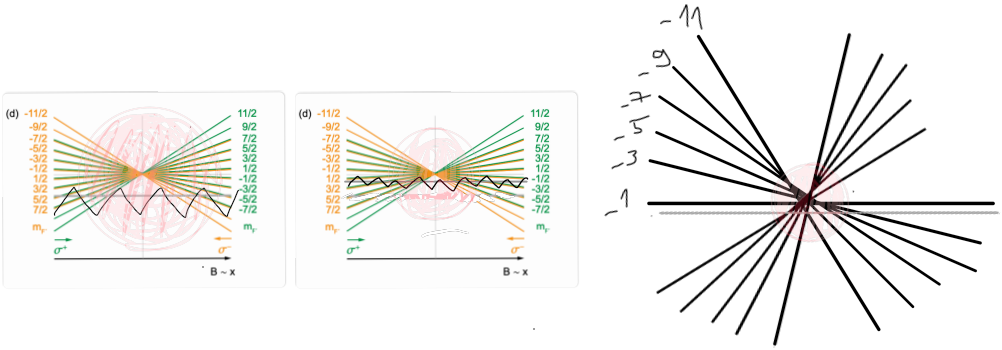

Figure 1.4: Caption

1.1.5.1 First step

1.1.5.2 Second step

1.1.6 Stir

Need a stir because :

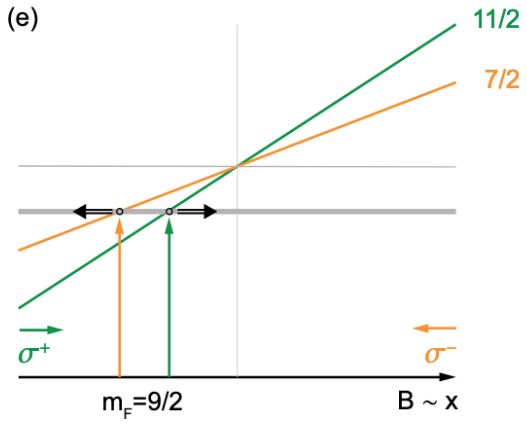

Figure 1.5: Caption

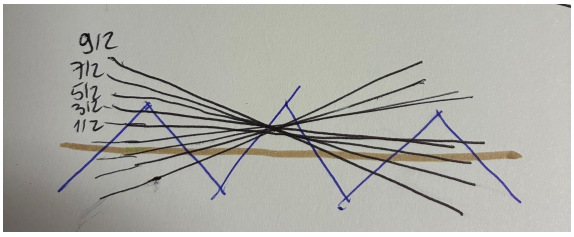

Figure 1.6: Caption

1.1.7 Narrow MOT

cf p.43 S.Stellmer thesis

1.1.7.1 Optimization of the narrow MOT (intensity, frequency, effect on the size of the cloud)

Include images of the cloud for different I and detuning ?

1.1.7.2 Optical setup

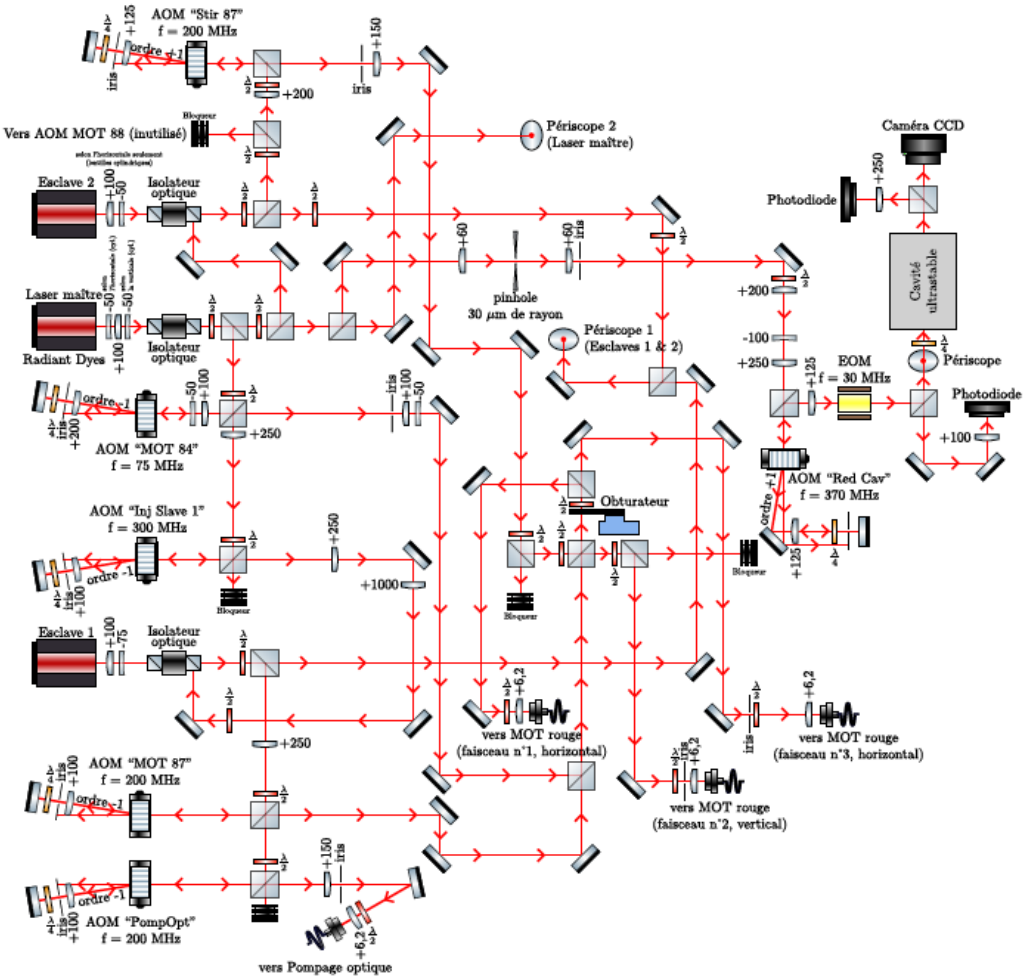

FIGURE 14 – Préparation des différents lasers rouges

Figure 1.7: Caption

1.1.8 ODT and evaporation

1.1.8.1 Charging the crossing

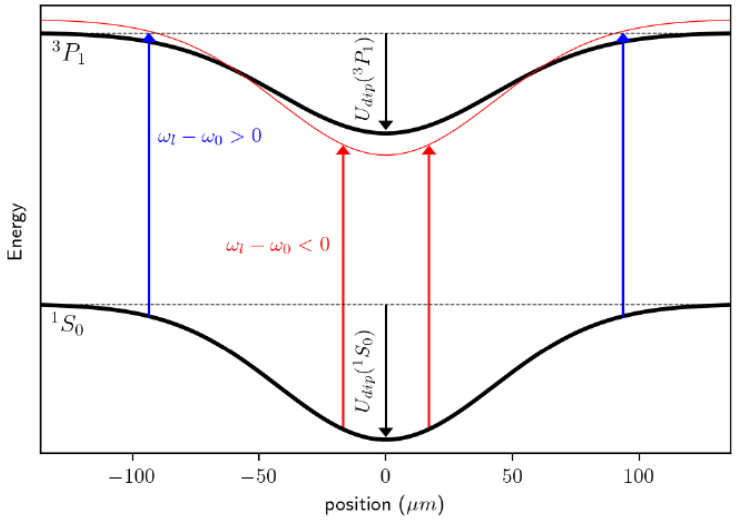

Figure 1.8: Caption

1.1.8.2 Optimization of the evaporation ramps : Dimple + reservoir, just reservoir, parameter to optimize (number of atoms, temperature)

Comment on the LS it does to each state

1.1.8.3 Optical setup

1.1.9 Optical pumping

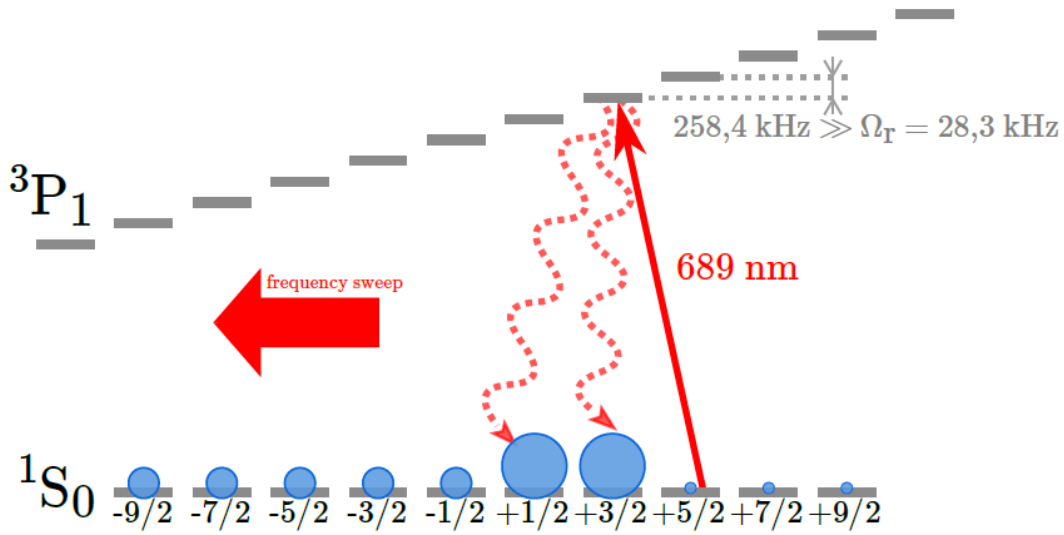

Figure 1.9: Caption

1.2 Spin measurement scheme

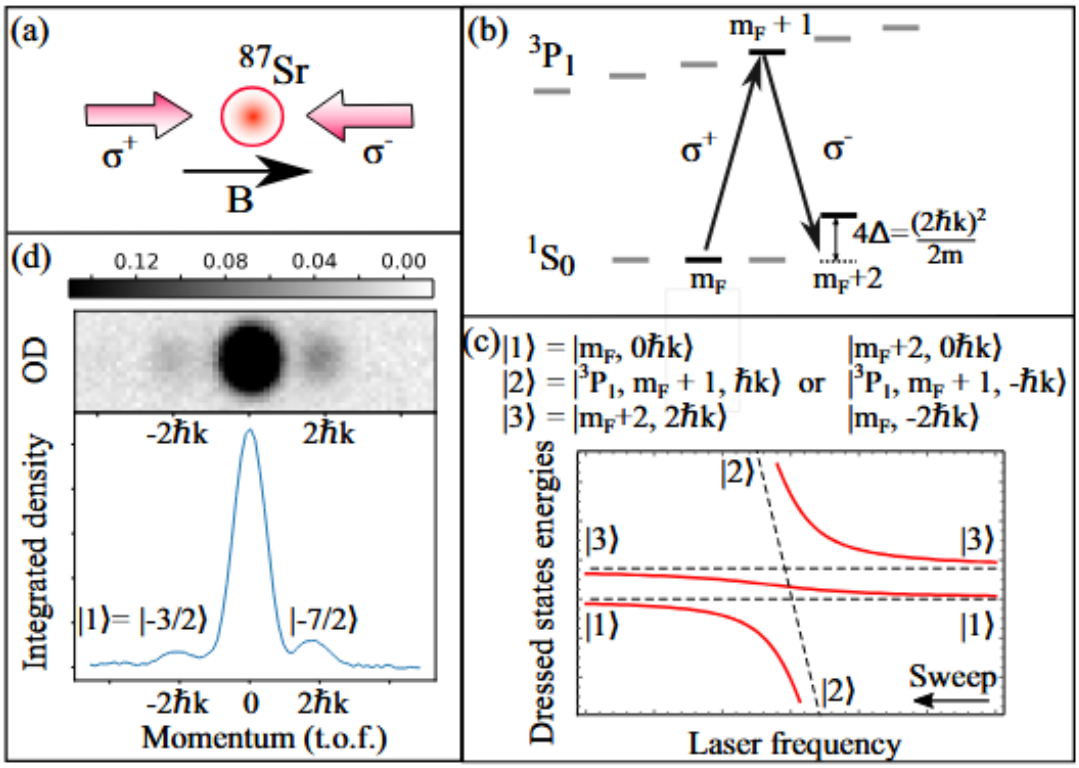

Figure 1.10: Caption

Chapter 2

Ramsey interferometers on qudit

2.1 Preparation of arbitrary dimension Hilbert space

2.1.1 Raman process

2.1.1.1 $\delta m_F = \pm 1$

2.1.1.2 $\delta m_F = \pm 2$

2.1.2 Moglabs chain without cavity

2.1.3 Purification of the laser spectrum with a FP cavity

blablablagtg

2.2 Interferometric sensing with multiple nuclear spin state

2.2.1 Driving long coherence time Rabi oscillations

2.2.1.1 Rabi oscillations

Comment on what the FP could add as a longer coherence time of the qubit

2.2.1.2 Interferometer of su(2) symmetry

2.2.1.3 Discussion on inhomogeneites

2.2.2 Measuring two quantites at a time

2.2.2.1 Physical principle

2.2.2.2 Results

2.2.3 Measuring two non commuting observables

2.2.3.1 Principle

2.3 SU(N) symmetry (ce qu'il faudrait pr la tester e.g densité gaz, alimentation bobines -¿ comment faire mieux que les chiffres actuels)

Chapter 3

Engineering highly entangled system of photoassociated 87Sr atoms

Engineering Dicke states

3.1 Introduction on photoassociation

3.1.1 Preamble on scattering theory

It is convenient in the case of the ^{87}Sr to approximate the electrons following the movement of the nuclei because of the mass ratio. In a Born-Oppenheimer picture we neglect the coupled terms between the kinetic energy of the electrons and the kinetic energy of the nuclei. In this manner we can study separately the radial and the angular part of the electronic movement.
As in the LANDAU-ZENER we will find the solutions of the 1D radial Schrödinger equation of the electrons

$$-\frac{\hbar^2}{2\mu}\left(\frac{1}{r^2}\frac{d^2\Psi_l}{dr^2}r^2 - \frac{l(l+1)}{r^2} + \hat{V}(r)\right)\Psi_l = E\Psi_l \tag{3.1}$$

- Ψ_l the eigenfunction - by approximating the scattering of the atoms as a sum of an incoming plane wave with a spherical scattered one - considered as plane wave at long distance -

$$\Psi_l = e^{i\mathbf{k}\cdot\mathbf{z}} + f(\theta)\frac{e^{ikr}}{r} \tag{3.2}$$

$f(\theta)$ a function that will tell the absorption of the scattered wave if the collision is elastic or inelastic. θ is the angle between the vector wore by the incoming wave with the vector wore by the scattered wave.

The solution at asymptotes contains the scattering part of the phenomenon studied on this subsection. To solve this hamiltonian we will take the results of [1] that

changes the solution basis to find a general solution of the hamiltonian 3.1.

$$\Psi_l = \frac{a_l}{r} sin(kr - \frac{l\pi}{2} + \delta_l) \tag{3.3}$$

with a_l a normalization factor and δ_l the phase acquired by the atoms at the distance at which they scatter.

Continuity of the wavefunction in every region should be respected. It gives

$$\delta_l \propto k^{2l+1} \tag{3.4}$$

For s-waves ($l = 0$), this express as

$$a = -\lim_{k\to 0} \delta_0/k \tag{3.5}$$

To understand how the atoms scatter we are going to express the scattered part of 3.2 as $\Psi_l - e^{ikz}$ in a spherical basis where the solutions are a sum on all the partial waves.

$$\Psi_l \simeq \frac{i}{2kr} \sum_{l=0}^{\infty} (2l+1) \left((-1)^l e^{-ikr} - S_l e^{ikr} \right) \tag{3.6}$$

with $S_l = e^{2i\delta_l}$ the scattering amplitude.

The final elastic cross section that tells the surface area of the scattering is

$$\sigma_{el} = \frac{\pi}{k^2} \sum_{l=0}^{\infty} (2l+1)|1 - S_l|^2 \tag{3.7}$$

For the inelastic collisions cross section reads as

$$\sigma_{inel} = \frac{\pi}{k^2} \sum_{l=0}^{\infty} (2l+1)(1 - |S_l|^2) \tag{3.8}$$

The term $1 - |S_l|^2$ quantifies the lost part of the incoming wave.

Equation 3.8 reveals that we need to introduce a new writing of $|S_l|^2$ with a complex term otherwise the inelastic cross section would be zero. Also it has to be inferior to one for losses.
At $l = 0$

$$S_0 = e^{2i\delta_0} \simeq 1 + 2i\delta_0 \tag{3.9}$$

By using the result of 3.5

$$1 + 2i\delta_0 \simeq 1 - 2ika \tag{3.10}$$

A direct result of these equations is that we can write a general scattering length as

$$a = a' + il_{opt} \tag{3.11}$$

a is what we call the scattering length and is the radius of the scattering cross section $\sigma_e = 4\pi|a|^2$. l_opt is the optical length, the radius of the inelastic scattering cross section $\sigma_{inel} = 4\pi/kl_{opt}$.

In ultracold gases, only s-wave atoms can collide because they do not have enough kinetic energy to pass the potential barrier of higher angular momentum states. It imposes that for fermions -by parity of the total wavefunction being antisymetric- only atoms with even angular momentum can collide meaning their spin is in a singlet state as in the case of ^{87}Sr. For bosons it is the contrary : from an even orbital wavefunction, the spin wavefunction should be antisymetric to collide.

3.1.2 What is photoassociation

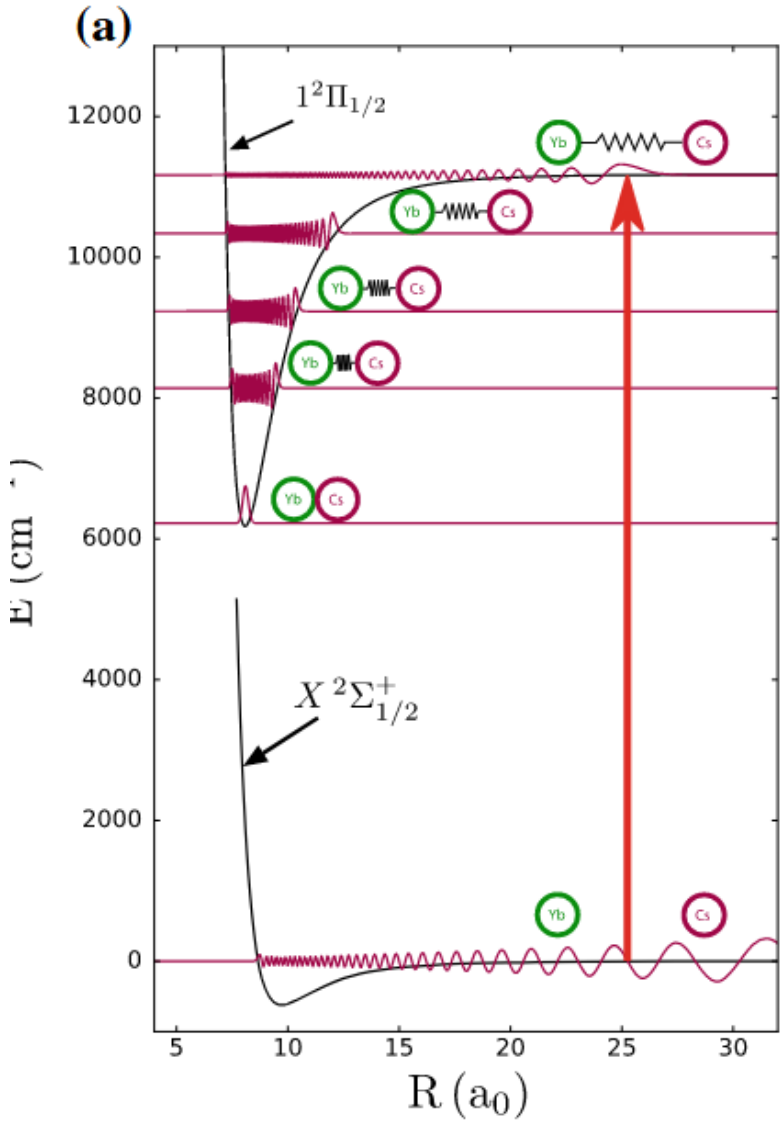

Figure 3.1: Caption

Photoassociating two atoms consists in bounding two colliding atoms with light that occurs mostly with two-body and three body losses.

As visible in 3.1 from a free state of a two-atoms system we couple them via a laser with a molecular vibrationnal state. In the case of spectroscopy we usually start with the least bounded state to have the atomic state reference. From that we sweep the atom frequency to adress the molecular states red detuned from the atomic line. The quantity that will testify there is two-body losses is the atom number remaining in the trap after a photoassociation pulse. The molecule leaves the trap by acquiring kinetic energy from the binding energy. The experimental proof of photoassociation is given by

$$\frac{dN}{dt} = -\beta N^2 - \Gamma N \tag{3.12}$$

β the fitted parameter of two-body losses ($\beta = \frac{K_2 V_e}{2}$, K_2 in comparison with [2]) the two-body loss rate, V_e the effective volume of the cloud $(2\pi)^{3/2}\sigma_x\sigma_y\sigma_z$ for a density Gaussian distribution and Γ the one-body losses rate. This latter is limited by the vacuum quality and the lifetime of the atoms in the trap.

PA is mostly used in Feschbach resonance field because determining the exact position of the vibrational states enables by changing the magnetic field to tune the scattering length of the atoms and thus the interactions in the system.

3.1.3 Molecular formalism/vocabulary (condon radius, optical length...)

Optical length characterizes the strength of the photoassociation rate

$$K_2 = \frac{4\pi\hbar}{\mu} n l_{opt} \tag{3.13}$$

μ the reduced mass of the two atoms. This rate represents the ratio of the atoms that are lossed by 2-body losses.

It contains the probability to transition from an initial vibrational i state to a final vibrational f state : **the Franck Condon factor** ([3])

$$F_{FC} = \left| \int_0^\infty \psi_i(r)\psi_f(r)dr \right|^2 \tag{3.14}$$

r the inter-nuclear distance. It depends directly with the overlap of the wavefunctions of the initial and final states. **The Condon radius** is the distance between the atoms for which this factor is maximum which also means that in a classical approach the atoms spend the most time at this position.

The good quantum numbers
We write the total angular momentum of the molecule $T = R + F = R + I + J$, F being the total spin of the two atoms $f_1 + f_2$, $J = j_1 + j_2$ is the angular momentum of the molecule that describes the spin-orbit coupling, and R the rotational angular

momentum of the molecule.

We define the projection of the different angular momentum on the inter-nuclear axis as

$$\Omega = \Lambda + \Sigma \tag{3.15}$$

with Λ the projection of the orbital momentum of the molecule on the internuclear axis and Σ the projection of the momentum spin.

M_T is the projection of the total angular momentum T onto a defined quantization axis.

For the rotational quantum number there is a parity of the total wavefunction that needs to be fulfilled. In addition there are only s-wave collisions in cold gases then the part of the wavefunction should be odd the spin one antisymetric

$$|\Psi\rangle = \left(|\phi_e\rangle_A |\phi_g\rangle_B + (-1)^R |\phi_e\rangle_B |\phi_g\rangle_A\right) \otimes |\chi\rangle \tag{3.16}$$

$|\phi_e\rangle$ and $|\phi_g\rangle$ are the electronic wavefunctions of the two atoms A and B in ground and excited state respectively, $|\chi\rangle$ is the spin wavefunction. It gives accessible values $R = 0, 2$ or 4...

For $^1S_0$ - $^3P_1$ molecular state there is a strong spin-orbit coupling that couples its related momentum to the internuclear axis (3.2), quantified by Ω and described as Hund's case (c)

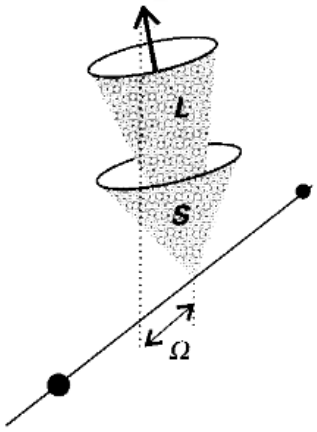

Fig. 11.4 A vector diagram for Hund's case (c), in which the spin–orbit coupling is very strong.

Figure 3.2: hund

The experiment presented in the following section is photoassociation in the $F = 11/2$ hyperfine state. We will focus in this state to simplify the discussion.
Say we have one atome in the $^1S_0$ state and one in the $^3P_1$ state: we can have a total spin of $J = 0, 1$ or 2. It gives possible values of total atomic angular momentum F:

$$\text{For } J = 0, \quad F = \frac{9}{2} \tag{3.17}$$

$$\text{For } J = 1, \quad F = \frac{7}{2}, \frac{9}{2}, \frac{11}{2} \tag{3.18}$$

$$\text{For } J = 2, \quad F = \frac{5}{2}, \frac{7}{2}, \frac{9}{2}, \frac{11}{2}, \frac{13}{2} \tag{3.19}$$

We have one atom with $f_1 = 9/2$ from the $^1S_0$ state and one in the $^3P_1$ state with $f_2 = 11/2$. The possible values of total angular momentum of the molecule are

$$\text{For } R = 0, \quad T = 1, 2, 3...10 \tag{3.20}$$

$$\text{For } R = 2, \quad T = 1, 2...12 \tag{3.21}$$

$$\text{For } R = 4, \quad T = 1, 2...14 \tag{3.22}$$

The initial $T^i = i_1 + i_2$ with $R = 0$ because we are in s-wave collisions. In respect with the parity $p = +1$ the possible values of T^i are $T^i = 0, 2, 4....$
As for atoms there are selection rules for transitions from a free state to a molecular state fixed by the angular momentum of the electrons. $\Delta J = 0, 1$ gives $\Delta T = 0, 1$ with $T = 0 \to T = 0$ forbidden.
In the end the accessible transitions in the first molecular excited state of the $f_1 = 11/2$ are

$$\text{For } R = 0, \quad T^f = 1, 2, 3...11 \tag{3.23}$$

$$\text{For } R = 2, \quad T^f = 1, 2...13 \tag{3.24}$$

$$\text{For } R = 4, \quad T^f = 1, 2...15 \tag{3.25}$$

$$... \tag{3.26}$$

There are 981 combinations of accessible (R, T^f) molecular states
Another element to describe the molecule is the symmetry of the orbital wavefunction. For an even wavefunction the exchange of the two atoms A and B does not change the sign of the wavefunction, as in left figures 3.3. We say the potential is **gerade**. The probability of finding electrons in between the two atoms is high compared to the **ungerade** potential where the odd wavefunction cancels the probability of finding electrons in between.

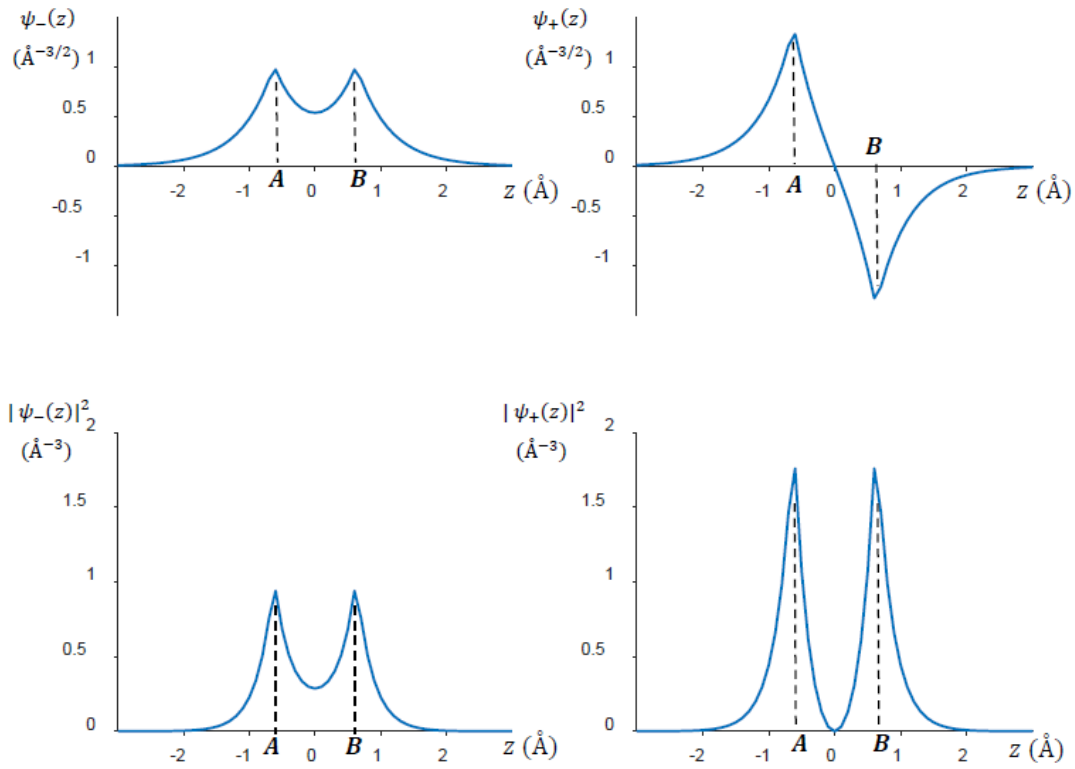

Figure 8.5 : Evolution le long de l'axe internucléaire Oz ($x=0, y=0$) des fonctions d'onde liante $|\psi_-\rangle$ et antiliante $|\psi_+\rangle$ et des densités de probabilité de présence de l'électron associées $|\psi_-|^2$ et $|\psi_+|^2$. La distance internucléaire est fixée à $R = 1{,}25$ Å (minimum de E_-).

Figure 3.3: u-g symmetry

3.1.4 External energy states

As seen in the subsection 3.1.1 in a molecular picture the hamiltonian express as in [2] by

$$\hat{H} = \frac{\hat{p_r}^2}{2\mu} + \frac{\hbar^2}{2\mu r^2} R\,(R+1) + \hat{V}_{BO} + \hat{H}_{HF} \tag{3.27}$$

with

$$\hat{V}_{BO} = \frac{-C_6}{r^6}\left(1 - \frac{\sigma^6}{r^6}\right) - s\frac{C_3^\Omega}{r^3} \tag{3.28}$$

$$\hat{H}_{\mathrm{hf}} = A\,(\mathbf{i}_1 \cdot \mathbf{j}_1) + B\,\frac{3(\mathbf{i}_1 \cdot \mathbf{j}_1)^2 + \frac{3}{2}(\mathbf{i}_1 \cdot \mathbf{j}_1) - i_1(i_1+1)\,j_1(j_1+1)}{2i_1(2i_1-1)\,2j_1(2j_1-1)} \tag{3.29}$$

$s = \pm 1$ for gerade and ungerade potentials respectively. The hyperfine term of the atom in ${}^1S_0$ is zero because its electronic angular momentum is zero. Only the hyperfine interaction of the atom with i_1, j_1 in ${}^3P_1$ counts.

3.1.4.1 WKB approximation

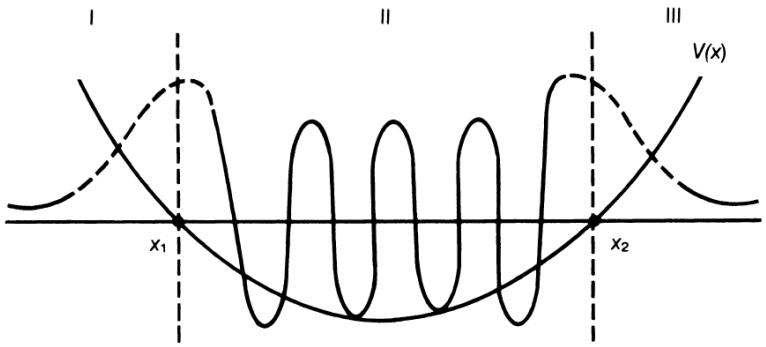

IGURE 2.1. Schematic diagram for behavior of wave function $u_E(x)$ in potential well $V(x)$ ith turning points x_1 and x_2.

Figure 3.4: Caption

3.1.4.2

3.1.5 Internal energy states

Leroy-Bernstein approx

3.2 About photoassociation on other species

3.2.1 Mass scaling (^{88}Sr)

^{88}Sr is a bosonic isotope of strontium with no hyperfine structure. The photoassociation spectrum is then simpler than the fermionic ones : only two potentials in the first excited molecular state 0_u and 1_u. Results have been presented in [4] where their fitting model gives the following potential expression

$$\hat{V}_{BO} \sim \frac{-C_{6,\Lambda}}{r^6} - \frac{C_3}{r^3} + \frac{C_J}{r^2} \tag{3.30}$$

for the two accessible potentials $\Lambda = 0, 1$.

Mass scaling method presented in [5] enables to predict the position of the vibrational states of the different istopoes of strontium.

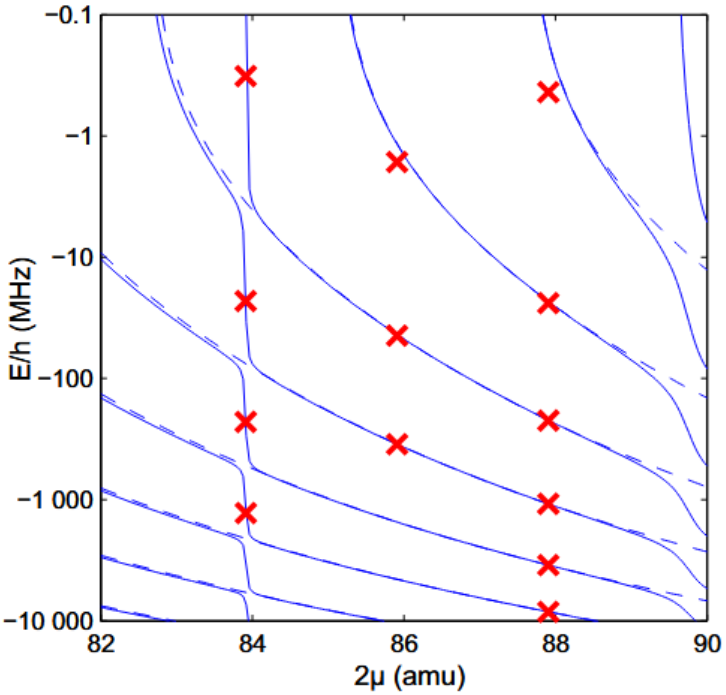

Figure 3.5: Caption

3.2.2 Ytterbium: hfs

As the ^{87}Sr the fermionic ^{173}Yb has a hyperfine structure that makes its molecular potential landscape more complex than many known species.

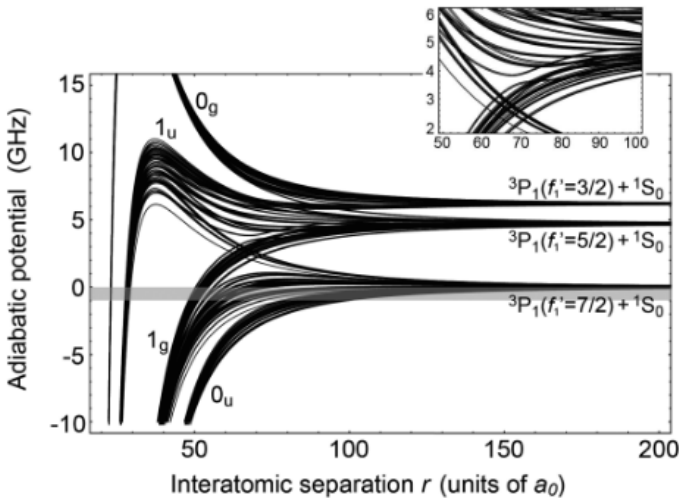

FIG. 2. Adiabatic molecular potentials for a $^{173}Yb_2$ dimer in the $^1S_0 + {}^3P_1$ channel as functions of the interatomic separation r. The molecular potentials for 205 different (T, F, R) configurations are displayed, which are accessible via PA from the initial s-wave colliding atoms in the $^1S_0 + {}^1S_0$ channel. At large r, the potentials converge to three asymptotic branches which correspond to excited atomic states with hyperfine numbers of $f_1' = 3/2,\ 5/2$, and $7/2$. Some of the potentials have a local minimum (inset), possibly hosting purely long-range bound states [14]. The energy offset is adjusted to the $f_1' = 7/2$ asymptote. The shaded region indicates the spectral range of our measurements.

Figure 3.6: Caption

^{171}Yb In their fitting model they consider the same interactions as in our case (expressed in equation 3.27) but without the hyperfine term.

3.3 Experimental setup

3.4 88Sr Results

Lopt, power broadening, thermal broadening...

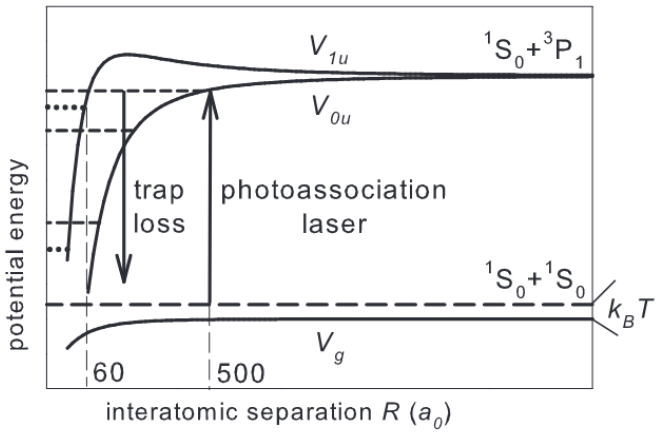

Figure 3.7: Caption

3.4.1 Technical issues of inhabilitation of photoassociation

3.4.1.1 Laser width

3.5 87Sr molecules

Lopt questions sur nb quantique / choix de pompage optique

3.5.1 Physical sources of inhabilitation of photoassociation

3.5.1.1 On F = 9/2 : predissociation

3.5.1.2 Coupling to more energetic state from the IR

3.5.1.3 Node of wavefunction for some vibrational states

3.5.2 Energy landscape of 87Sr-87Sr molecules

Conclusion

Bibliography

[1] J. Dalibard, "Les interactions entre atomes dans les gaz quantiques,"

[2] J. H. Han, J. H. Kang, M. Lee, and Y.-i. Shin, "Photoassociation spectroscopy of ultracold ^{173}Yb atoms near the intercombination line," *Physical Review A*, vol. 97, p. 013401, Jan. 2018. arXiv:1710.03072 [physics].

[3] A. Guttridge, *Photoassociation of Ultracold CsYb Molecules and Determination of Interspecies Scattering Lengths*. Springer Theses, Cham: Springer International Publishing, 2019.

[4] T. Zelevinsky, M. M. Boyd, A. D. Ludlow, T. Ido, J. Ye, R. Ciurylo, P. Naidon, and P. S. Julienne, "Narrow Line Photoassociation in an Optical Lattice," *Physical Review Letters*, vol. 96, p. 203201, May 2006. Number: 20 arXiv:physics/0602135.

[5] B. J. Reschovsky, B. P. Ruzic, H. Miyake, N. C. Pisenti, P. S. Julienne, and G. K. Campbell, "Narrow-line photoassociation spectroscopy and mass-scaling of bosonic strontium," Oct. 2018. arXiv:1808.06507 [physics].

Appendix A

Algorithms